X-ray Activated Near-infrared Persistent Luminescent Probe for Deep-tissue and Renewable *In Vivo* Bioimaging

Zhenluan Xue, Xiaolong Li, Youbin Li, Mingyang Jiang, Hongrong Liu, Songjun Zeng* and Jianhua Hao*

Prof. S. J. Zeng, Z. L. Xue, X. L. Li, Y. B. Li, M. Y. Jiang, Prof. H. R. Liu
College of Physics and Information Science and Key Laboratory of Low-dimensional Quantum Structures and Quantum Control of the Ministry of Education, Synergetic Innovation Center for Quantum Effects and Applications, Hunan Normal University, Changsha, Hunan 410081 (China)
E-mail: songjunz@hunnu.edu.cn
Prof. J. H. Hao

Department of Applied Physics, The Hong Kong Polytechnic University, Hong Kong (China)
E-mail: jh.hao@polyu.edu.hk

Keywords: NIR persistent luminescence, X-ray activation, *in vivo* whole-body bioimaging, deep-tissue activation and imaging, renewable bioimaging

Near-infrared (NIR) persistent luminescence nanoparticles (PLNPs) are considered as a new alternative optical probe due to the free of autofluorescence benefited from the self-sustained emission after excitation and high signal-to-noise ratio. However, the NIR-emitted PLNPs always present short decayed time and require the excitation of ultraviolet or visible light with short penetrable depth, remarkably hindering their applications for *in vivo* long-term tracking and imaging *in vivo*. Therefore, it is important to develop NIR-emitted PLNPs with *in vivo* activation nature by new excitation source with deeper penetrating depth. Here, we propose a new type of X-ray activated $ZnGa_2O_4$: Cr PLNPs (X-PLNPs) with efficient NIR persistent emission and rechargeable activation feature, in which both the excitation and emission possess high penetrable nature *in vivo*. These X-PLNPs exhibit long-lasting up to 6 h NIR emissions at 700 nm after the stoppage of X-ray excitation source. More importantly, the designed X-PLNPs can be readily reactivated by a soft X-ray excitation source with low excitation power (45 kVp, 0.5 mA) to restore *in vivo* bioimaging signals even at 20 mm depth.

Renewable *in vivo* whole-body bioimaging was also successfully achieved via intravenous injection/oral administration of X-PLNPs after in situ X-ray activation. Up to now, this is the first time to demonstrate NIR-emitted PLNPs could be recharged by X-ray light for deep tissue *in vivo* bioimaging, which paves the way for *in vivo* renewable bioimaging using PLNPs and makes the PLNPs more competitive in bioimaging area.

1. Introduction

Currently, owing to the efficient storage of excitation energy in energy traps, PLNPs with long-lasting NIR persistent emission after cessation of excitation light have attracted great research interest for optical imaging.[1-3] PLNPs with efficient persistent emission have been widely applied in security signs, medical diagnostics, safety indication and fiber-optic thermometers.[2,4] In comparison with the traditional nanoprobes needed in situ external excitation during imaging, such as upconversion nanocrystals,[5] metal nanoclusters[6] and quantum dots,[7] PLNPs with no need for in situ activation property leading to zero-autofluorescence were emerged as ideal optical probes for *in vivo* bioimaging.[8] Recently, Scherman's and co-workers demonstrated $Ca_{0.2}Zn_{0.9}Mg_{0.9}Si_2O_6$: Eu^{2+}, Mn^{2+}, Dy^{3+} PLNPs with NIR afterglow can be served as optical probes for *in vivo* bioimaging without any external illumination source during imaging.[9] Furthermore, they reported $CaMgSi_2O_6$: Eu^{2+}, Mn^{2+}, Pr^{3+} PLNPs with improved persistent optical nature.[10] Additionally, a new type of $Zn_3Ga_2Ge_2O_{10}$ PLNPs doped with Cr^{3+} with a super-long NIR persistent luminescence after sunlight activation was proposed by Liu.[4] An ultra-long NIR afterglow more than 1000 h of $LiGa_5O_8$: Cr^{3+} PLNPs was realized by using ultraviolet (UV) as an excitation source.[11] More interestingly, NIR-emitted $Zn_{2.94}Ga_{1.96}Ge_2O_{10}$: Cr^{3+}, Pr^{3+} PLNPs as optical probes were applied for *in vivo* bioimaging for more than 7 h after intravenous injection without an external illumination source.[1] Therefore, PLNPs with tissue-penetrable NIR emission have the potential as bioimaging probes with deep tissue penetration and high signal-to-noise ratio.

In spite of the NIR-emitted PLNPs possessing no in situ excitation and enhanced signal-to-noise ratio characteristics, these probes still suffer from the drawback of short observation time for *in vivo* bioimaging, hindering its applications in *in vivo* long-time tracking and tumor assessments usually needing a window of days or even weeks.[12] Specifically, most of the PLNPs are activated by short tissue penetrating UV light, which can not be able to reactive the PLNPs uptaken by biotissue in living animals.[9-10,13-15] Recently, Han's group reported that $ZnGa_2O_4$: Cr and $SiO_2/ZnGa_2O_4$: Cr nanocomposites with NIR-emission could be recharged in a mouse model under a white light-emitting diodes (LED).[16-17] In addition, Scherman and co-workers successfully verified that $ZnGa_{1.995}Cr_{0.005}O_4$ PLNPs can be reactivated *in vivo* using red LED.[18] However, although visible photons possess rechargeable persistent luminescent feature for PLNPs, its application for *in vivo* tracking is still hindered by its limitation penetration of visible light. Thus, it is of great importance to develop NIR-PLNPs with rechargeable optical nature *in vivo* by a deep tissue penetrating source.

Recent years have witnessed the rapid development of utilizing X-ray as an innovative excitation source for imaging technique.[19-20] Energetic electrons from X-ray are able to stimulate luminescent centers in the various phosphors and then generate light.[19-20] As we known, the results of some fluorescent materials, such as lanthanide-doped nanoparticles, gold nanoclusters, metal-organic frameworks and radioluminescent nanomaterials under X-ray excitation were similar to that by traditional optical excitation.[19,21-25] Furthermore, compared to the traditional optical excitation (UV/visible/NIR), X-ray possesses competitive advantages of weaker scattering and deeper penetration depth in tissues, and image reconstruction simplification for optical tomography.[20,26] Recently, an X-ray excited optical imaging probe based on $NaGdF_4$: Eu^{3+} host was reported by Kennedy.[27] Xing and co-workers demonstrated that Yb/Er doped $NaYF_4$ nanoparticles presented shortwave infrared emission for bioimaging by X-ray irradiation.[20] Based on the above results, we speculate that

PLNPs can be also activated by X-ray and then produce NIR persistent luminescence for *in vivo* deep tissue bioimaging, which could provide higher sensitivity information and improve efficiency of diagnose disease. However, there is still no report about PLNPs that can be reactivated in living animals for *in vivo* bioimaging by using X-ray as an excitation source. Thus, developing X-ray rechargeable persistent luminescence nanoplatform by combining the advantages of X-ray excitation and NIR persistent emission, opens the door for achieving deeper tissue and higher sensitivity optical bioimaging with unprecedented spatial resolution.

Herein, as proof of concept, we selected $ZnGa_2O_4$: Cr PLNPs as model for X-ray activated NIR persistent emission. *In vitro* and *in vivo* NIR persistent luminescent bioimaging based on these X-PLNPs were demonstrated. More importantly, the X-PLNPs were also repeatedly charged *in vivo* by X-ray at deep location up to 20 mm. These results revealed that X-ray could be acted as a new excitation source for persistent renewable bioimaging with deep penetration-depth based on NIR-PLNPs.

2. Results and disscusion

2.1. Characterization and X-ray activated NIR persistent luminescence of X-PLNPs

X-ray activated NIR persistent luminescence based on X-PLNPs is illustrated in **Scheme 1**, and rechargeable *in vivo* deep tissue imaging was realized after stopping X-ray irradiation. The X-PLNPs were synthesized by a sol-gel method combined with a further calcination. The X-ray diffraction results (Figure S1, Supporting Information) reveal that the synthesized X-PLNPs present cubic phase structure, matching with the standard cubic phase of $ZnGa_2O_4$ (JCPSD NO.: 38-1240). And no other impurity peaks were detected, indicating the successful incorporation of Cr^{3+} into host matrix. The morphology observed by transmission electron microscopy (TEM, **Figure 1**a) of X-PLNPs presents particle-like shape with nanosize. Selected area electron diffraction (SAED) pattern of X-PLNPs (inset of Figure 1a) clearly

shows the (111), (200) and (220) diffraction rings, further validating the formation of cubic phase $ZnGa_2O_4$. The high-resolution TEM (HRTEM) image shows the lattice distance was 4.82 Å (Figure S2, Supporting Information), matching well with *d* spacing of (111) crystal plane of cubic phase. The atomic compositions of Zn, C, Cu, Ga and O elements in the X-PLNPs were detected by energy-dispersive X-ray spectrometry (EDS) (Figure S3, Supporting Information). Notably, Cu and C are ascribed to TEM grid. In order to reveal the optical properties of Cr^{3+}, the excitation and emission spectra of X-PLNPs were measured. As shown in Figure 1b, excitation spectrum of X-PLNPs exhibits two characteristic excitation bands ranging from 350-487 nm and 487-650 nm, which are attributed to the electrons transitions of $^4A_2$ $^4T_1$, and $^4A_2$ $^4T_2$ of Cr^{3+}, respectively. The emission spectrum of X-PLNPs shows efficient NIR emission located at 700 nm, originating from ^2E $^4A_2$ transition of Cr^{3+} under the 365 nm excitation at room temperature.[28]

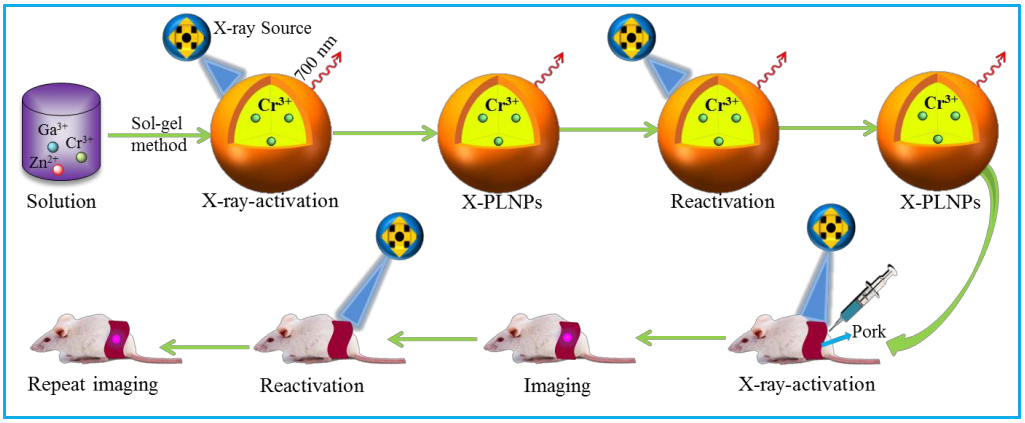

Scheme 1. A schematic diagram for *in vivo* NIR persistent rechargeable deep tissue bioimaging under X-ray excitation.

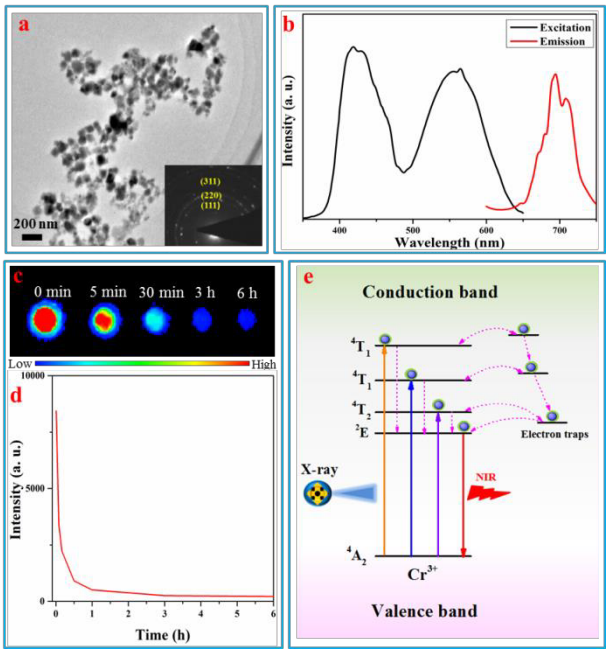

Figure 1. a) TEM image of X-PLNPs, inset: SAED, b) excitation (black curve) and emission (red curve) spectra of X-PLNPs powders at room temperature, c) *in vitro* decay NIR persistent luminescence imaging of X-PLNPs after ceasing X-ray (5 min, 45 kVp) irradiation, d) *in vitro* charged decay curve of X-PLNPs, e) mechanism scheme of persistent luminescence under X-ray excitation, the dotted-line arrows and solid-line arrows represent electron transfer processes and optical transitions, respectively.

To detect NIR afterglow signal, X-PLNPs were first studied after 20 min irradiation with a 365 nm UV lamp by a CCD equipped on the multi-modal imaging system (Scheme S1). The results of *in vitro* phantom imaging and corresponding afterglow decay curve (Figure S4, Supporting Information) revealed that the X-PLNPs could be activated by UV light and NIR persistent luminescence signal sustained for 10 h after ceasing the UV light. In addition, as demonstrated in Figure S5 (Supporting Information), X-PLNPs also exhibit a long-lasting *in vivo* bioimaging (7 h) after pre-excitation by UV light. These results indicate that X-PLNPs can be *ex vivo* charged by UV light for *in vitro/in vivo* imaging, which is similar to the previous report.[3] Furthermore, in order to validate the X-ray activated NIR persistent emission, *in vitro* phantom imaging and decay curve based on X-PLNPs at different decay

time after pre-excitation by X-ray (45 kVp, 5 min) were performed. As demonstrated in Figure 1c and 1d, the signals of NIR persistent luminescence are gradually decreased with increasing the decay time after ceasing excitation. Notably, the NIR persistent emission can be observed and visualized for more than 6 h, unambiguously indicating that X-ray can be also used as an efficient excitation source for PLNPs. The X-ray induced NIR persistent luminescence mechanism of $ZnGa_2O_4$: Cr PLNPs was shown in Figure 1e, which is similar to the result of UV. Upon X-ray irradiation, Cr^{3+} ions absorb the incident energy and the electrons are promoted from the valence band to the conduction band, attributed to the electron transition of $^4A_2$ $^4T_1$.[1,4] Then the excited electrons are captured by electron traps. When the electron traps are corresponded to the levels of $^4T_1$ and $^4T_2$ of Cr^{3+}, the free electrons will be captured through a tunneling process.[1] After the stoppage of the X-ray excitation, the persistent luminescence was occurred by the recombination of electrons and holes, resulting in an intense NIR persistent luminescence (^2E $^4A_2$).[4,18]

2.2. Repeated persistent luminescence imaging irradiated by X-ray

In order to study the effect of accelerating voltages and exposure times on the intensity of NIR afterglow, X-PLNPs were systematically studied under different accelerating voltages (25, 35, 45 kVp) of X-ray and exposure times. When the exposure time is kept for 5 min (Figure S6, Supporting Information), the intensity of NIR persistent luminescence is enhanced with increasing X-ray accelerating voltage from 25 kVp to 45 kVp. Meanwhile, maintaining the accelerating voltage at 45 kVp of X-ray (Figure S7, Supporting Information), the NIR persistent luminescent intensity is improved with promoting exposure time. In addition, the results of *in vivo* imaging (Figure S8, S9, Supporting Information) based on X-PLNPs further prove that high X-ray accelerating voltage and long exposure time contribute to more efficient NIR persistent luminescence. In order to evaluate the feasibility of renewable NIR persistent luminescence by X-ray, the NIR emission and decays of X-PLNPs were repeated for four cycles after irradiated with 45 kVp X-ray for 5 min. As exhibited in **Figure 2**, the NIR

persistent luminescence based on X-PLNPs is renewable by X-ray excitation after four cycles. These results validate that X-PLNPs can be readily recharged by X-ray and exhibit the long-lasting NIR persistent luminescence, which has potential application in rechargeable *in vivo* NIR persistent bioimaging.

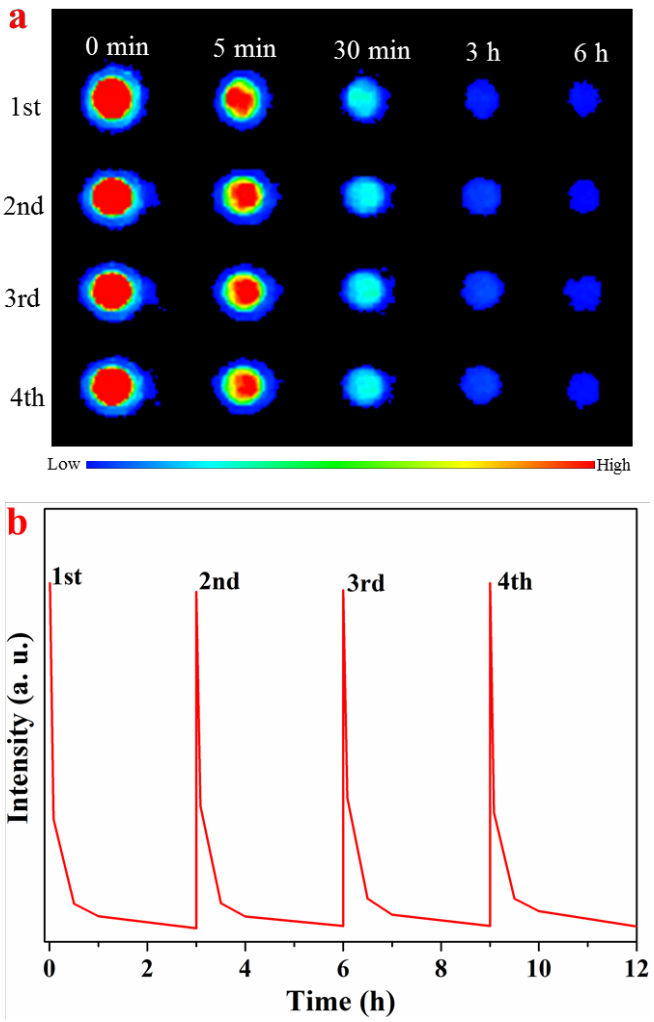

Figure 2. Rechargeable NIR persistent luminescent properties of the nanosized $ZnGa_2O_4$: Cr X-PLNPs. a) Repeated *in vitro* phantom NIR persistent luminescence imaging achieved by a CCD camera at different decay times after stopping X-ray excitation (5 min, 45 kVp), b) NIR afterglow decay curves of X-PLNPs for four repeated imaging after the stoppage of X-ray irradiation.

2.3. *In vitro* deep tissue activation and imaging

To compare deep tissue activation and imaging ability, *in vitro* phantom imaging of X-PLNPs covered with various thicknesses (0, 1, 3, 5, 10, and 20 mm) pork slabs was obtained by using X-ray and UV as excitation sources (**Figure 3**a). As demonstrated in Figure 3b, distinct NIR afterglow signals of X-PLNPs could still be observed even increasing pork slabs from 0 mm to 20 mm depth after X-ray excitation. However, no signal can be detected when the thickness of pork slab is more than 3 mm under UV irradiation (Figure 3c). Furthermore, the corresponding intensity curves (Figure 3d) further demonstrate that X-ray as an excitation source possesses higher biotissue-penetrable depth than UV. As we known, the capacity of in situ rechargeable is vital for long-term persistent luminescence bioimaging.

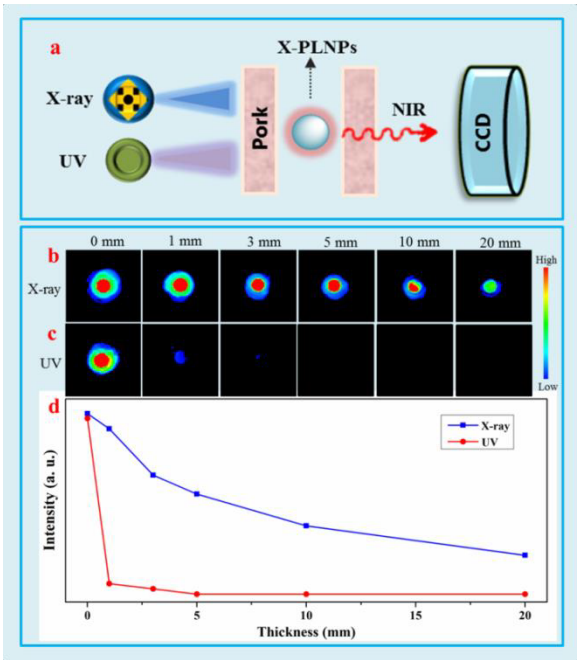

Figure 3. a) Schematic diagram of NIR persistent luminescence for deep tissue imaging activated by X-ray/UV, b) *in vitro* phantom imaging of X-PLNPs covered with different thicknesses of pork tissues (0, 1, 3, 5, 10, and 20 mm) under X-ray and c) UV excitation, respectively, d) variation curves of signal intensity under different thicknesses by X-ray/UV irradiation.

2.4. *In vivo* deep tissue activation and imaging

Prior to *in vivo* bioimaging, the cytotoxicity of X-PLNPs was tested and the results revealed that the cell viability was greater than 90% by even adding high content of X-PLNPs up to 1000 μg/mL (Figure S10, Supporting Information), indicating the low cell toxicity of the X-PLNPs. Encouraged by low cell toxicity and the high biotissue-penetrable depth nature of NIR/X-ray light, *in vivo* deep tissue activation and repeated imaging of a subcutaneous Kunming mouse covered with different thicknesses (10, 15, and 20 mm, Figure S11, Supporting Information) of pork slabs were performed after ceasing X-ray irradiation. As shown in Figure 4a, a NIR persistent signal can be detected in subcutaneous injection site under 10 mm depth of pork slab. Although the signal intensity is decreased when increasing the thickness from 10 mm to 20 mm, the NIR persistent signal (Figure 4b, 4c) can still be observed even at 20 mm depth. These results imply that utilizing X-ray as PLNPs excitation source possesses deeper tissue penetrable depth than that from previous reports by using UV, visible, and NIR laser (Table S1, Supporting Information).[17,29] In addition, the corresponding *in vivo* deep tissue repeated imaging and decay curves were also presented in **Figure 4** and Figure S12 (Supporting Information), indicating X-ray as an excitation source having both deep biotissue-penetrable depth and rechargeable *in vivo* bioimaging nature. Recently, Xing and co-workers developed *in vivo* X-ray induced luminescence imaging based on rare-earth nanoprobes by using X-ray with power of 320 kVp and 12.5 mA (Table S1, Supporting Information).[20] However, in this study, *in vivo* renewable bioimaging was achieved by using a multi-modal imaging system operating at only 45 kVp and 0.5 mA. Therefore, the needed X-ray dosage in our experiment is lower about 17.8 times than Xing's report.[20] Thus, X-PLNPs with rechargeable NIR persistent luminescence under low powered X-ray irradiation can be regarded as optimal optical probes for bioimaging with deep penetration depth, high sensitive and signal-to-noise. It also should be pointed out that using high power X-ray excitation source (for example 320 kVp and 12.5 mA) may result in remarkable promoted penetration depth and deeper tissue detection in *in vivo*.

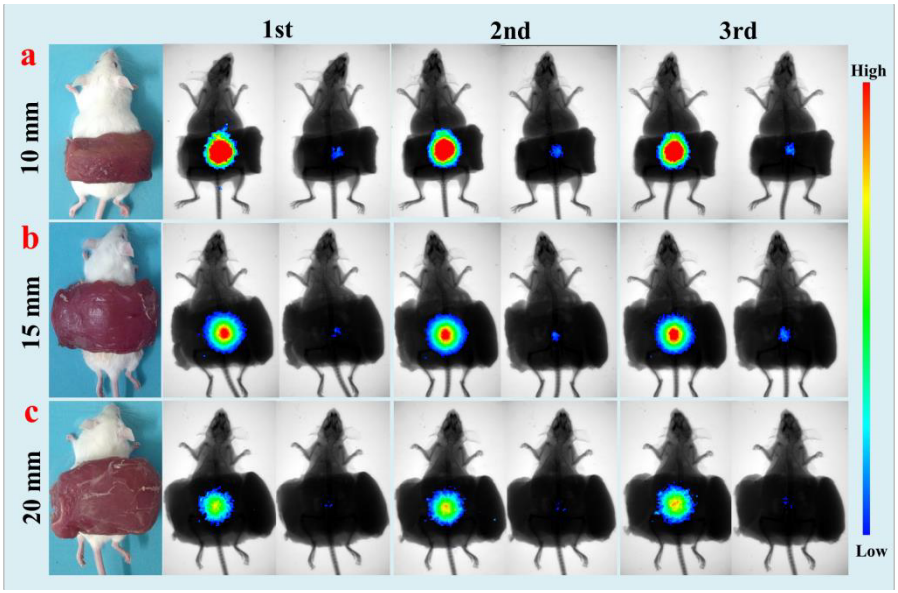

Figure 4. Renewable *in vivo* persistent bioimaging of a Kunming mouse after subcutaneous injection of X-PLNPs covered with different thicknesses of pork slabs a) 10 mm, b) 15 mm and c) 20 mm after the stoppage of X-ray excitation.

2.5. Renewable *in vivo* whole-body NIR bioimaging via X-ray excitation

Encouraged by the aforementioned deep tissue activation and imaging feature, X-PLNPs aqueous solution was exposed to a UV lamp and then intravenously injected into a Kunming mouse for *in vivo* whole-body bioimaging (Figure S13a, Supporting Information). As shown in Figure S13b (Supporting Information), An obvious NIR persistent signal can be detected in liver region after treatment and maintained for 3 h. Figure S13c (Supporting Information) shows the NIR persistent luminescence decay curve of X-PLNPs, which is matched well with the result of *in vivo* bioimaging. However, after NIR signal decayed, we didn't observe NIR signal by reactivation via UV light (Figure S14b, Supporting Information), impeding their applications in *in vivo* long-term tracking and bioimaging. Interestingly, a significant NIR persistent luminescence signal (Figure S14c, Supporting Information) can be detected after irradiated via low powered X-ray, indicating the rechargeable nature of X-PLNPs *in vivo* X-ray light. This findings reveal that X-ray as a light source possesses much higher penetrating depth for renewable bioimaging than UV. To further demonstrate the renewable *in*

vivo whole-body bioimaging, X-PLNPs without UV irradiation was intravenously injected into another mouse (**Figure 5**), *in vivo* whole-body bioimaging was captured after in situ X-ray excitation. As demonstrated, compared to pre-excitation, a significant NIR persistent signal was observed in liver region after in situ X-ray excitation and gradually decayed (Figure 5b). Moreover, after recharged by X-ray, *in vivo* renewable whole-body bioimaging was successfully achieved (Figure 5b). The NIR persistent luminescence of X-PLNPs could be recharged constantly in situ more than four times (Figure S15, Supporting Information). Additionally, to further detect the biodistribution of X-PLNPs, the isolated organs achieved from the intravenously injected mice was performed for imaging under in situ X-ray excitation. As shown in Figure S16 (Supporting Information), the NIR signal intensity in liver was the strongest among organs, indicating X-PLNPs were mainly accumulated in liver.

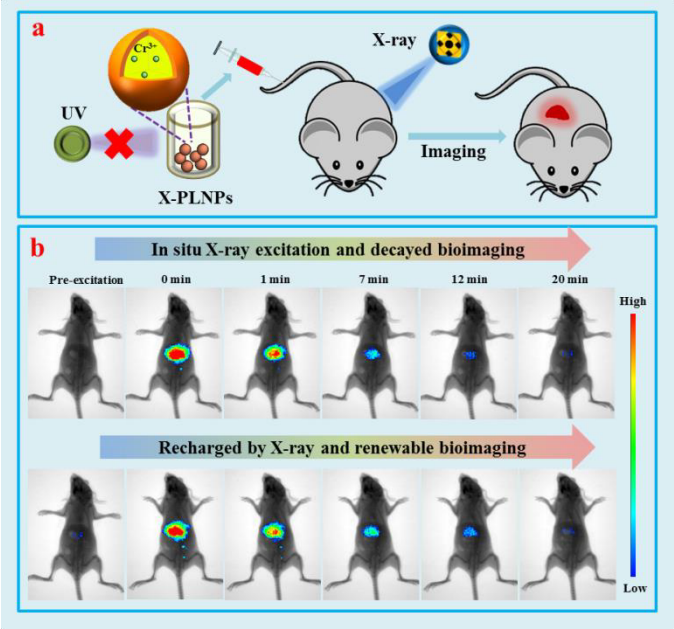

Figure 5. a) A schematic representation of *in vivo* whole-body persistent bioimaging of mouse after intravenous injection with X-PLNPs by in situ X-ray excitation, b) *in vivo* decayed and renewable whole-body bioimaging of intravenously injected mouse after ceasing X-ray excitation.

Moreover, *in vivo* bioimaging of mouse by oral administration of X-PLNPs after in situ X-ray irradiation was also performed (**Figure 6**a). After 8 h oral administration, intestines and stomach region presented a significant NIR persistent signal and lasted for about 50 min (Figure 6b), and the repeatable bioimaging was achieved after X-ray excitation. The corresponding decay curve of four repeated bioimaging (Figure S17, Supporting Information) further indicated the rechargeable of X-PLNPs *in vivo*. Furthermore, *ex vivo* imaging of main organs collected from the oral administration mouse was achieved. As shown in Figure S18 (Supporting Information), only intestines and stomach presented NIR signal, indicating X-PLNPs were assembled in intestines and stomach. Therefore, the designed X-PLNPs exhibited low toxicity and can be oral gavage for *in vivo* long-term bioimaging after in situ X-ray excitation. Based on the above results, the designed X-PLNPs can be used as ideal probes for *in vivo* persistent optical bioimaging and be recharged by in situ X-ray irradiation for renewable and long-term bioimaing.

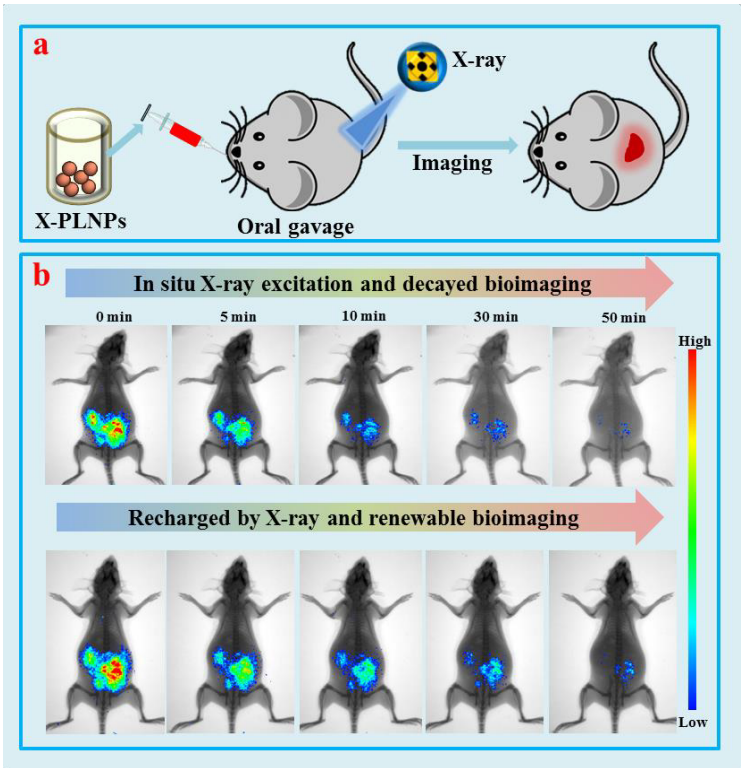

Figure 6. a) A schematic diagram of *in vivo* bioimaging of mouse with oral administration of X-PLNPs after in situ X-ray excitation, b) rechargeable *in vivo* NIR persistent bioimaging of mouse at different time via oral gavage of X-PLNPs after stoppage of X-ray excitation.

3. Conclusion

In summary, we designed an X-ray activated $ZnGa_2O_4$: Cr X-PLNPs with efficient long-lasting NIR persistent emission for *in vivo* whole-body and renewable bioimaging. The X-PLNPs with NIR persistent luminescence at around 700 nm is ascribed to ^2E $^4A_2$ transition of Cr^{3+}. The results of X-ray induced *in vitro* repeated imaging indicate X-PLNPs can be reactivated by X-ray. Due to the negligible scattering and deep penetration depth characteristics of X-ray, *in vivo* deep tissue (even at 20 mm depth) and renewable bioimaging were achieved by low power excitation of X-ray. Moreover, after intravenous injection and oral administration of X-PLNPs, repeatable *in vivo* whole-body bioimaging was also successfully achieved after ceasing X-ray excitation. This is the first demonstration of renewable NIR persistent luminescence for *in vivo* deep tissue bioimaging by using low power X-ray, which can surpass the bioimaging performance using the conventional persistent luminescence nanoparticles pumped by photon. These findings will pave the way for designing new NIR-emitted PLNPs for *in vivo* long-term tracking and high sensitive bioimaging.

4. Experimental Section

Chemicals and materials: $Ga(NO_3)_3$: $Zn(NO_3)_2$, $Cr(NO_3)_3$, nitric acid, citric acid and ammonium hydroxide were gotten from Sinopharm Chemical Reagent Co., China.

Synthesis of $ZnGa_2O_4$: Cr X-PLNPs: The $ZnGa_2O_4$: 1%Cr X-PLNPs were synthesized by a citrate sol-gel approach with a subsequent calcination. In a typical experiment,[1] $Ga(NO_3)_3$, $Zn(NO_3)_2$ and $Cr(NO_3)_3$ were dissolved in de-ionized water to form homogenous solution and then mixed together at designed molar ratio under vigorously stirring, followed by the

addition of 1.5 mmol citric acid solution. Ammonia hydroxide was added the above mixture for reaching a pH of to 5.0. The mixed solution was constantly stirred under 60 °C until most of water was evaporated. Subsequently, the obtained solution was transferred in a vacuum oven (DZF 2B) and kept 75 °C until the solution from a sol to a gel. The final gel was heated at 130 °C for 4 h and then maintained at 200 °C for 12 h to obtain black porous materials. After annealed (1000 °C) for 3 h, the black porous materials were turn into white powders.

In order to obtain nanosized X-PLNPs, the $ZnGa_2O_4$: Cr was wet ground for 1 h by additional of little ethanol. Then NaOH solution (5 mmol) was used to disperse the fine X-PLNPs by means of sonication for 1 h. After that, the obtain mixture was vigorously stirred for 24 h. To remove the large sized particles, the acquired colloidal solution was centrifuged (5000 rpm) for 30 min. The suspension liquid was centrifuged (10000 rpm) for 10 min for collecting the precipitate. In order to obtain hydrophilic X-PLNPs, the precipitate was further treated by using polyethylene glycol (PEG).[28] In brief, 5 mg X-PLNPs were dispersed in de-ionized water by sonication for 2 h. 45 mg PEG was added into the mixture and then stirred for 20 h in the dark. For removing the redundant PEG, the resulting modified X-PLNPs were washed four times with de-ionized water.

Characterization: The X-ray diffraction (XRD) spectrum of X-PLNPs was performed on a diffractometer (D8 Discover Bruker) equipped with Cu Ka radiation (A =1.5418 A) at 40 kV and 40 mA. The morphology and microstructure of sample were characterized by using transmission electron microscopy (TEM, FEI Tecnai F20) provided an Energy-dispersive X-ray spectrometry (EDS), selected area electron diffraction (SAED) and high-resolution TEM (HRTEM) operating at an accelerating voltage of 200 kV. The luminescence and excitation spectra of X-PLNPs were recorded via a Zolix Analytical Instrument (fluoroSENS 9000 A) at room temperature. The *in vivo*/*in vitro* persistent luminescent imaging based on

X-PLNPs was performed in a multi-modal imaging system (Bruker *In Vivo* FX Pro, Scheme S1) equipped with a X-ray source.

Cytotoxicity evaluation: The cytotoxicity of modified X-PLNPs was tested by a 3-(4, 5-dimethylthiazol-2-yl)-2, 5 diphenyl-tetrazolium bromide (MTT) assays.[5(c)] In a typical procedure, human embryonic kidney 293 (Hek293) cells were incubated with Dulbecco's Modified Eagle Medium (DMEM) supplemented with heat-inactivated 10% fetal bovine serum, 1% penicillin and streptomycin and then were transferred into 96-well plates and cultured at 37℃ under 5% CO_2. After 4 h, the X-PLNPs at expected contents (0, 100, 300, 600, 1000 μg/mL) were added to the culture medium and incubated for 24 h. Subsequently, the cell viability was tested by MTT method.

Persistent luminescence imaging under UV excitation: For *in vitro* imaging, X-PLNPs were transferred into a 96-well plate and then were exposed to a UV lamp (365 nm) for 20 min. The persistent luminescence signals were recorded by a multi-modal imaging system (Bruker *In Vivo* FX Pro). A Kunming mouse was anesthetized with pentobarbital sodium aqueous solution (100 μL, 10 wt%) via intraperitoneal injection. The X-PLNPs solution (250 μL, 3 mg/mL) was pre-irradiated with a UV lamp for 20 min before bioimaging. Subsequently, the pre-irradiated X-PLNPs solution was subcutaneously injected to the anesthetized mouse for *in vivo* persistent luminescence bioimaging. All animal procedures obey the guidelines of the Laboratory Animal Center of Hunan Province.

NIR-recharged in vitro/in vivo imaging by X-ray: A 96-well plate with X-PLNPs was placed in a multi-modal imaging system equipped with an X-ray source for *in vitro* imaging. When the irradiation time was maintained 5 min, the accelerating voltage of X-ray was 25, 35, 45 kVp, respectively. Similarly, kept X-ray 45 kVp, and the exposure time was 1, 3 and 5 min, respectively. Additionally, the four repeated *in vitro* imaging based on X-PLNPs by using 45 kVp X-ray for 5 min was performed. The current of all measurements was 0.5 mA.

NIR-recharged in vitro/in vivo deep tissue imaging: To study the feasibility of X-ray-induced persistent luminescence for deep tissue-penetration depth, *in vitro* imaging of a 96-well plate with X-PLNPs covered with pork muscle tissues at different thicknesses (0, 1, 3, 5, 10, 20 mm) was carried out under UV/X-ray (45 kVp, 5 min) excitation. Additionally, in order to obtain the *in vivo* simulated deep tissue recharging imaging, a Kunming mouse after the subcutaneous injection (250 μL, 10 mg/mL) site covered with 10, 15 and 20 mm pork muscle tissues was performed by using a multi-modal imaging system. Digital pictures of pork slabs were taken by a digital camera.

In vivo whole-body bioimaging via intravenous and oral administration: To further evaluate the possibility of X-PLNPs as nanoprobes for *in vivo* whole-body bioimaging, X-PLNPs aqueous solution (150 μL, 4 mg/mL) was irradiated by a UV lamp (365 nm) for 20 min before intravenously injected into the anesthetized mouse. *In vivo* bioimaging was obtained by using a multi-modal *in vivo* imaging system at expected time points after administration.

Another Kunming mouse with intravenously injected of un-activated X-PLNPs aqueous solution (150 μL, 4 mg/mL) was used for *in vivo* whole-body bioimaging by in situ X-ray excitation. The injected mouse was charged/recharged by X-ray (45 kVp, 5 min) for *in vivo* NIR persistent luminescence bioimaging. Additionally, a Kunming mouse was treated with X-PLNPs aqueous solution via oral gavage for *in vivo* persistent luminescence bioimaging.

Supporting Information

Supporting Information is available from the Wiley Onling Library or from the author.

Acknowledgments

This work was supported by the National Natural Science Foundation of China (21671064), Scientific Research Fund of Hunan Provincial Education Department (13B062), CAS/SAFEA International Partnership Program for Creative Research Teams, and Supported by Hunan Provincial Innovation Foundation For Postgraduate (CX2016B204).

Received: ((will be filled in by the editorial staff))
Revised: ((will be filled in by the editorial staff))
Published online: ((will be filled in by the editorial staff))

References

[1] A. Abdukayum, J. T. Chen, Q. Zhao, X. P. Yan, *J. Am. Chem. Soc.* **2013**, *135*, 14125.

[2] T. Matsuzawa, Y. Aoki, N. Takeuchi, Y. Murayama, *J. Electrochem. Soc.* **1996**, *143*, 2670.

[3] A. Bessière, S. Jacquart, K. Priolkar, A. Lecointre, B. Viana, D. Gourier, *Optics Express* **2011**, *19*, 10131.

[4] Z. W. Pan, Y. Y. Lu, F. Liu, *Nat. Mater.* **2012**, *11*, 58.

[5] a) D. L. Ni, W. B. Bu, S. J. Zhang, X. P. Zheng, M. Li, H. Y. Xing, Q. F. Xiao, Y. Y. Liu, Y. Q. Hua, L. P. Zhou, W. J. Peng, K. Zhao, J. L. Shi, *Adv. Funct. Mater.* **2014**, *24*, 6613; b) F. Wang, X. G. Liu, *J. Am. Chem. Soc.* **2008**, *130*, 5642; c) Z. G. Yi, X. L. Li, Z. L. Xue, X. Liang, W. Lu, H. Peng, H. R. Liu, S. J. Zeng, J. H. Hao, *Adv. Funct. Mater.* **2015**, *25*, 7119; d) J. Zhou, Z. Liu, F. Y. Li, *Chem. Soc. Rev.* **2012**, *41*, 1323; e) L. Cheng, C. Wang, L. Z. Feng, K. Yang, Z. Liu, *Chem. Rev.* **2014**, *114*, 10869; f) D. M. Yang, P. A. Ma, Z. Y. Hou, Z. Y. Cheng, C. X. Li, J. Lin, *Chem. Soc. Rev.* **2015**, *44*, 1416; g) S. J. Zeng, Z. G. Yi, W. Lu, C. Qian, H. B. Wang, L. Rao, T. M. Zeng, H. R. Liu, H. J. Liu, B. Fei, J. H. Hao, *Adv. Funct. Mater.* **2014**, *24*, 4051; h) J. Zhou, Z. Liu, F. Y. Li, *Chem. Soc. Rev.* **2012**, *41*, 1323; (i) Y. S. Liu, D. T. Tu, H. M. Zhu, X. Y. Chen, *Chem. Soc. Rev.* **2013**, *42*, 6924.

[6] E. C. Dreaden, A. M. Alkilany, X. Huang, C. J. Murphy, M. A. El-Sayed, *Chem. Soc. Rev.* **2012**, *41*, 2740d9.

[7] I. L. Medintz, H. T. Uyeda, E. R. Goldman, H. Mattoussi, *Nat. Mater.* **2005**, *4*, 435.

[8] W. G. Yan, F. Liu, Y. Y. Lu, X. J. Wang, M. Yin, Z. W. Pan, *Optical Express,* **2010**, *18*, 20215-20221.

[9] Q. L. Masne de Chermont, C. Chaneac, J. Seguin, F. Pelle, S. Maitrejean, J. P. Jolivet, D. Gourier, M. Bessodes, D. Scherman, *Proc. Natl. Acad. Sci. U.S.A.* **2007**, *104*, 9266.

[10] T. Maldiney, A. Lecointre, B. Viana, A. Bessière, M. Bessodes, D. Gourier, C. Richard, D. Scherman, *J. Am. Chem. Soc.* **2011**, *133*, 11810.

[11] F. Liu, W. Yan, Y. J. Chuang, Z. Zhen, J. Xie, Z. Pan, *Sci. Rep.* **2013**, *3*, 1554.

[12] F. Liu, Y. J. Liang, Z. W. Pan, *Phys. Rev. Lett.* **2014**, *113*, 177401.

[13] F. Clabau, X. Rocquefelte, S. Jobic, P. Deniard, M. H. Whangb, A. Garcia, T. Le Mercier, *Chem. Mater.* **2005**, *17*, 3904.

[14] L. C. V. Rodrigues, J. Holsa, M. Lastusaari, M. C. F. C. Felinto, H. F. Brito, *J. Mater. Chem. C* **2014**, *2*, 1612.

[15] L. C. V. Rodrigues, H. F. Brito, J. Holsa, R. Stefani, M. C. F. C. Felinto, M. Lastusaari, T. Laamanen, L. A. O. Nunes, *J. Phys. Chem. C* **2012**, *116*, 11232.

[16] Z. J. Li, Y. W. Zhang, X. Wu, X. Q. Wu, R. Maudgal, H. W. Zhang, G. Han, *Adv. Sci.* **2015**, *2*, 1500001.

[17] Z. J. Li, Y. W. Zhang, X. Wu, L. Huang, D. S. Li, W. Fan, G. Han, *J. Am. Chem. Soc.* **2015**, *137*, 5304.

[18] T. Maldiney, A. Bessière, J. Seguin, E. Teston, S. K. Sharma, B. Viana, A. J. J. Bos, P. Dorenbos, M. Bessodes, D. Gourier, D. Scherman, C. Richard, *Nature Materials* **2014**, *13*, 418.

[19] G. Pratx, C. M. Carpenter, C. Sun, R. P. Rao, L. Xing, *Optics Letters* **2010**, *35*, 3345.

[20] D. J. Naczynski, C. Sun, S. Türkcan, C. Jenkins, A. L. Koh, D. Ikeda, G. Pratx, L. Xing, *Nano Lett.* **2015**, *15*, 96.

[21] A. Kamkaew, F. Chen, Y. H Zhan, R. L. Majewski, W. B. Cai, *ACS. Nano.* **2016**, *10*, 3918.

[22] C. Wang, O. Volotskova, K. Lu, M. Ahmad, C. Sun, L. Xing, W. Lin, *J. Am. Chem. Soc.* **2014**, *136*, 6171.

[23] Y. Osakada, G. Pratx, C. Sun, M. Sakamoto, M. Ahmad, O. Volotskova, Q. Ong, T. Teranishi, Y. Harada, L. Xing, B. Cui, *Chem. Commun. (Cambridge)* **2014**, *50*, 3549.

[24] C. Sun, G. Pratx, C. M. Carpenter, H. G. Liu, Z. Cheng, S. S. Gambhir, L. Xing, *Adv. Mater.* **2011**, *23*, H195.

[25] C. M. Carpenter, C. Sun, G. Pratx, R. Rao, L. Xing, *Med. Phys.* **2010**, *37*.

[26] H. Y. Chen, T. Moore, B. Qi, D. C. Colvin, E. K. Jelen, D. A. Hitchcock, J. He, O. T. Mefford, J. C. Gore, F. Alexis, J. N. Anker, *ACS. Nano.* **2013**, *7*, 1178.

[27] L. Sudheendra, G. K. Das, C. Q. Li, D. Stark, J. Cena, S. Cherry, I. M. Kennedy, *Chem. Mater.* **2014**, *26*, 1881.

[28] Y. C. Lu, C. X. Yang, X. P. Yan, *Nanoscale*, **2015**, *7*, 17929.

[29] Q. Q. Zhan, J. Qian, H. J. Liang, G. Somesfalean, D. Wang, S. He, Z. G. Zhang, S. Andersson-Engels, *ACS. Nano.* **2011**, *5,* 3744.

A new type of X-ray activated persistent luminescent probe with near-infrared emission was demonstrated for the first time. And rechargeable *in vivo* deep-tissue bioimaging by soft X-ray is achieved, providing a new possibility for *in vivo* renewable bioimaging using persistent luminescent nanoparticles.

NIR persistent luminescence, X-ray activation, *in vivo* whole-body bioimaging, deep-tissue activation and imaging, renewable bioimaging

Zhenluan Xue, Xiaolong Li, Youbin Li, Mingyang Jiang, Hongrong Liu, Songjun Zeng*and Jianhua Hao*

X-ray Activated Near-infrared Persistent Luminescent Probe for Deep-tissue and Renewable *In Vivo* Bioimaging

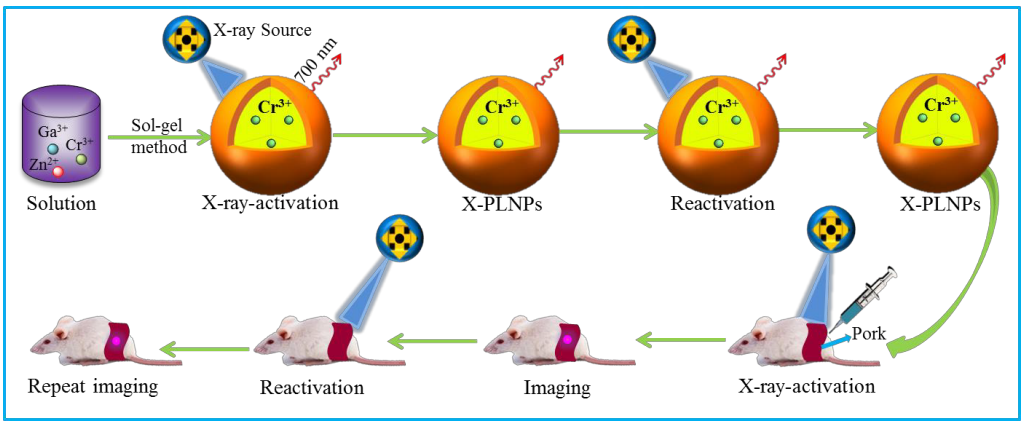

SUPPORTING INFORMATION

X-ray Activated Near-infrared Persistent Luminescent Probe for Deep-tissue and Renewable *In Vivo* Bioimaging

Zhenluan Xue, Xiaolong Li, Youbin Li, Mingyang Jiang, Hongrong Liu, Songjun Zeng* and Jianhua Hao*

Prof. S. J. Zeng, Z. L. Xue, X. L. Li, Y. B. Li, M. Y. Jiang, Prof. H. R. Liu

College of Physics and Information Science and Key Laboratory of Low-dimensional Quantum Structures and Quantum Control of the Ministry of Education, Synergetic Innovation Center for Quantum Effects and Applications, Hunan Normal University, Changsha, Hunan 410081 (China)

E-mail: songjunz@hunnu.edu.cn

Prof. J. H. Hao

Department of Applied Physics, The Hong Kong Polytechnic University, Hong Kong (China)

E-mail: jh.hao@polyu.edu.hk

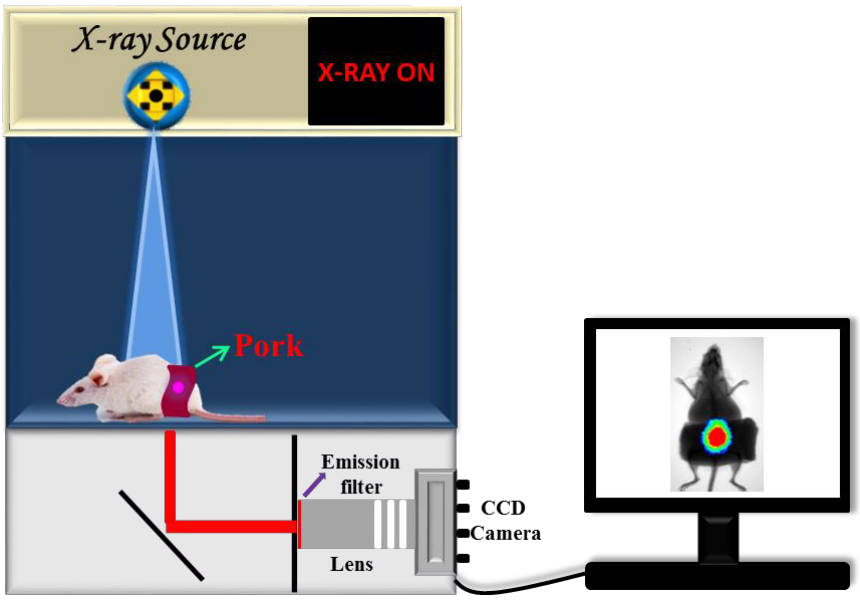

Scheme S1. Schematic of a multi-modal imaging system for *in vivo* rechargeable bioimaging by X-ray excitation.

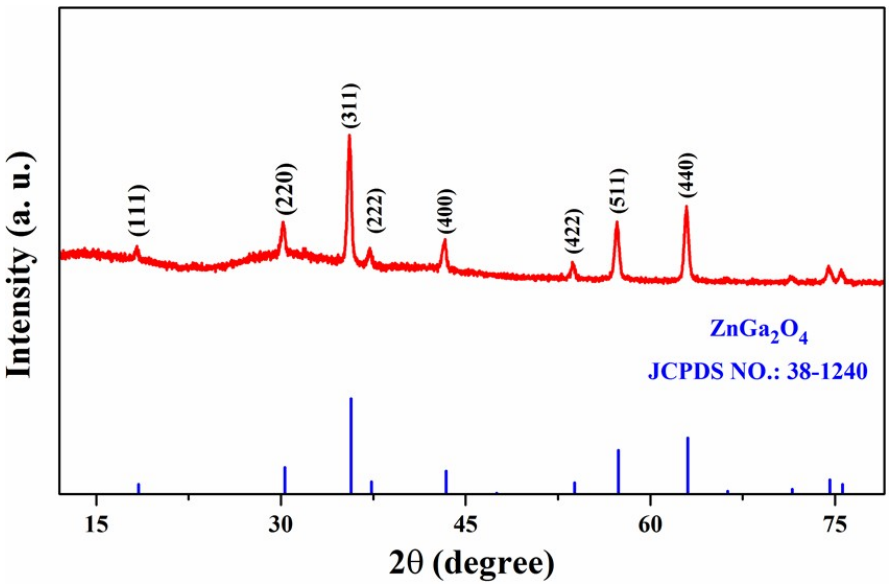

Figure S1. XRD pattern of $ZnGa_2O_4$: Cr X-PLNPs (red line). Blue line spectrum presents the standard data of the cubic phase $ZnGa_2O_4$ (JCPDS NO.: 38-1240).

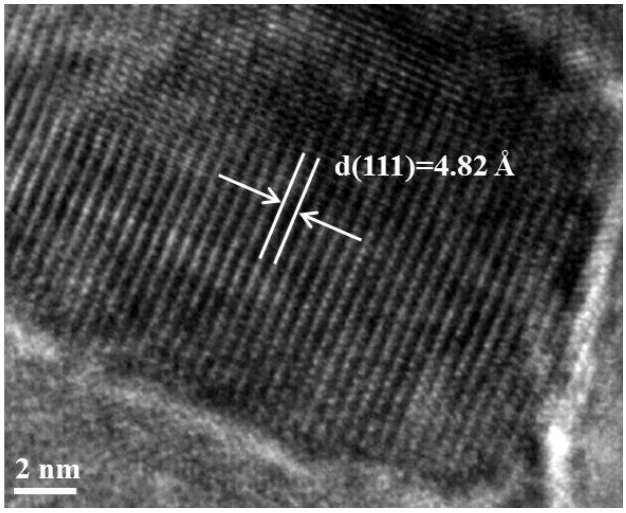

Figure S2. HRTEM of $ZnGa_2O_4$: Cr X-PLNPs.

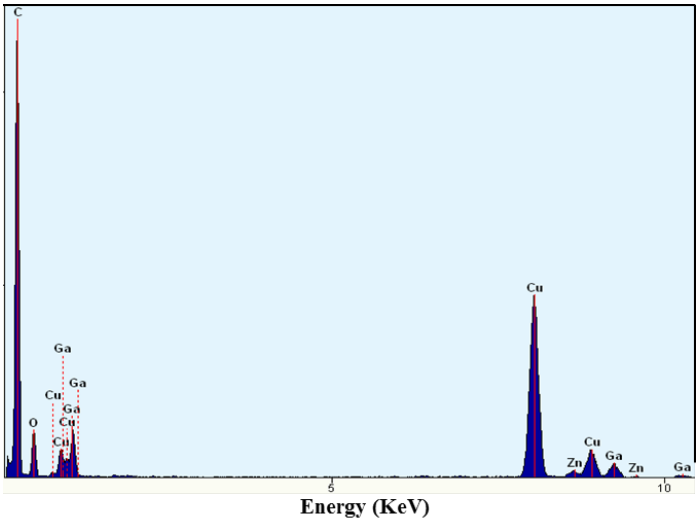

Figure S3. EDS spectrum of $ZnGa_2O_4$: Cr X-PLNPs.

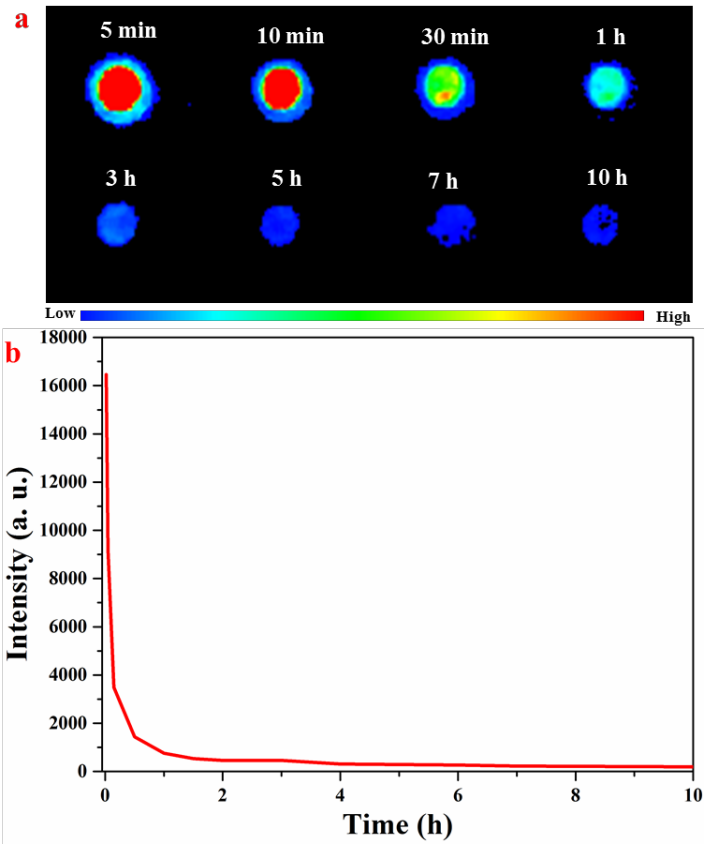

Figure S4. (a) *In vitro* NIR afterglow decay images and (b) decay curve of X-PLNPs at different times after stopping UV lamp irradiation.

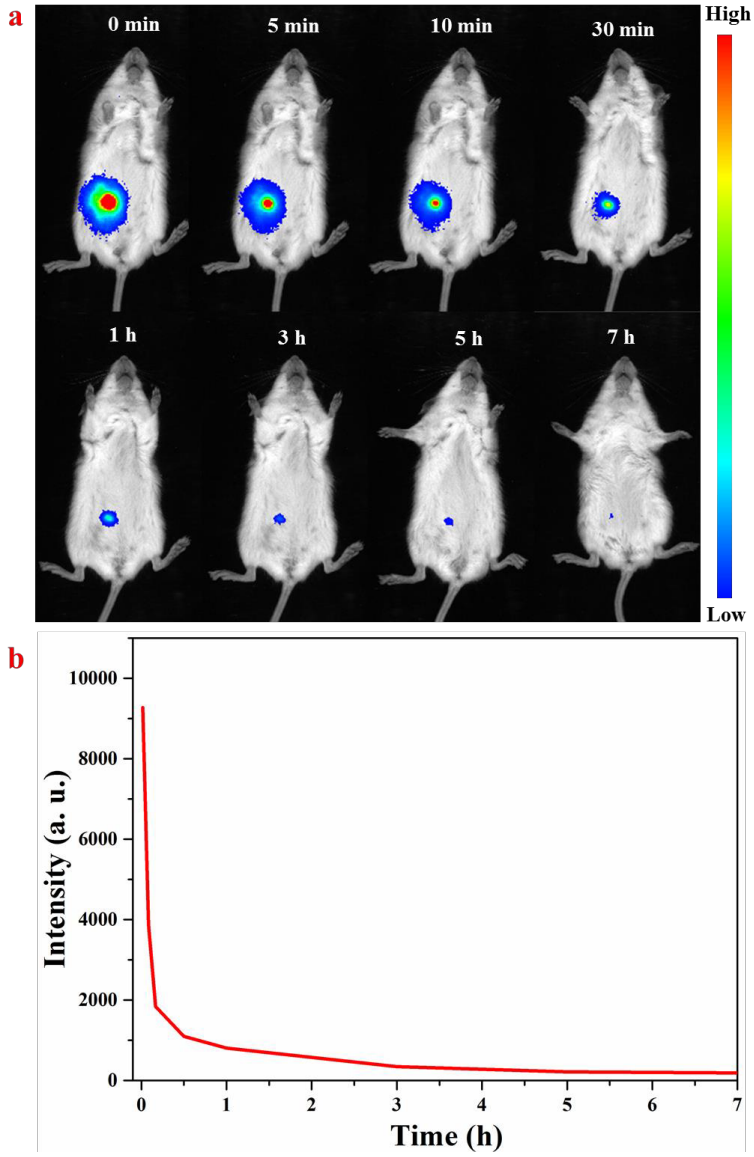

Figure S5. (a) *In vivo* NIR persistent luminescence bioimaging and (b) the corresponding decay curves of a Kunming mouse after subcutaneously injected of X-PLNPs under UV excitation.

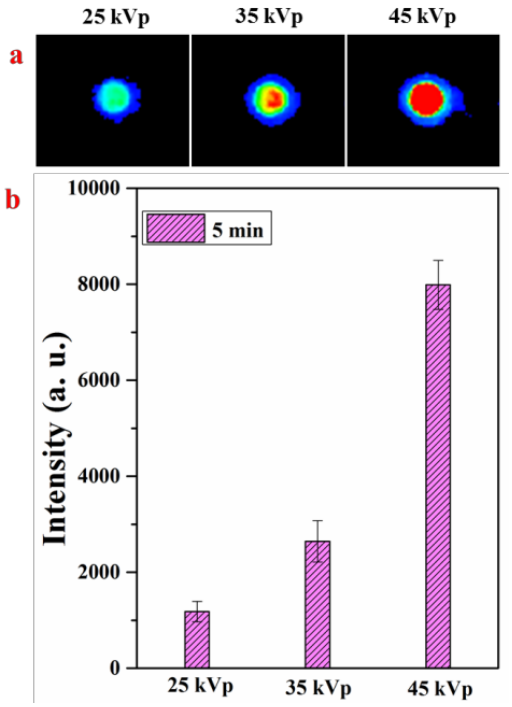

Figure S6. (a) *In vitro* NIR persistent luminescence imaging of X-PLNPs excited by 45 kVp X-ray with different irradiation times (1, 3, 5 min), (b) the corresponding intensity of *in vitro* NIR afterglow imaging.

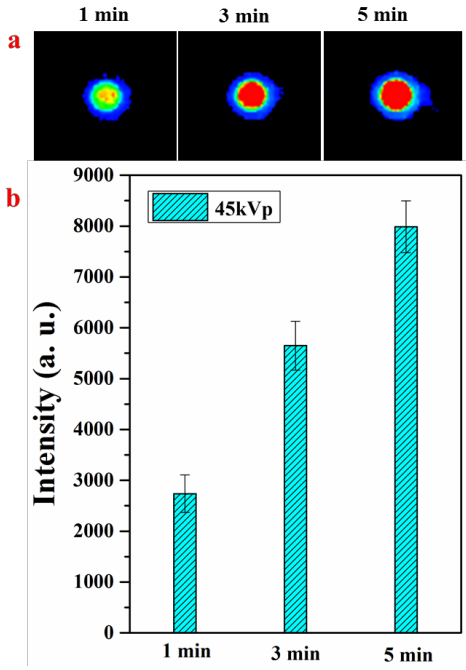

Figure S7. (a) *In vitro* NIR persistent luminescence imaging of X-PLNPs excited for 5 min by different accelerating voltages of X-ray (25, 35, 45 kVp), (b) the corresponding intensity of of *in vitro* NIR afterglow imaging.

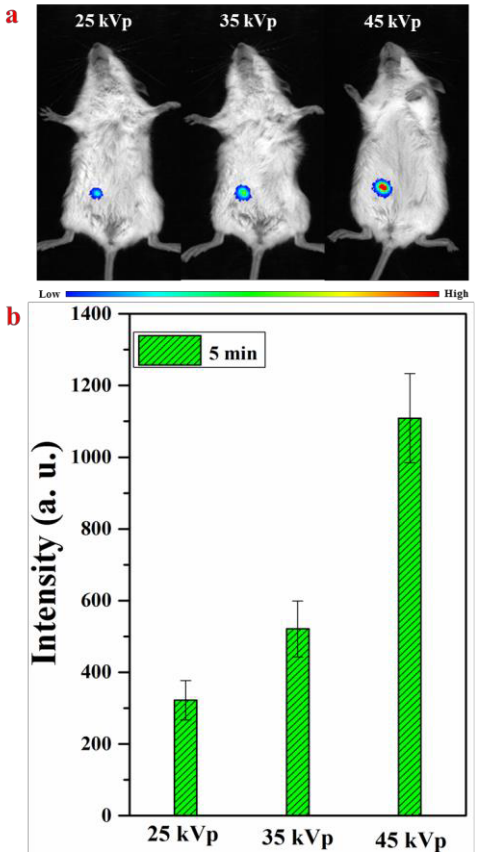

Figure S8. (a) *In vivo* NIR afterglow bioimaging (b) intensity based on X-PLNPs with activation for 5 min under different voltages of X-ray (25, 35, 45 kVp).

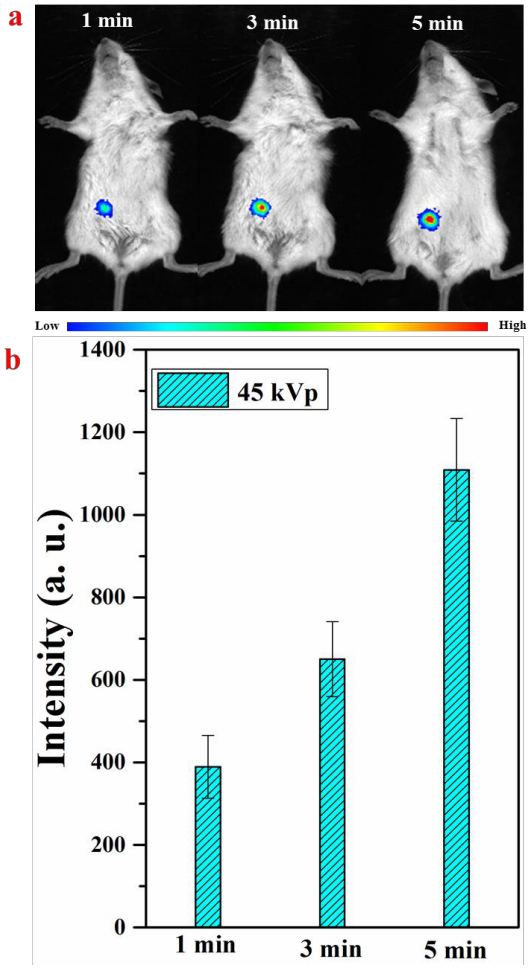

Figure S9. (a) *In vivo* NIR afterglow bioimaging and (b) intensity based on X-PLNPs activated by 45 kVp X-ray with different irradiation times (1, 3, 5 min).

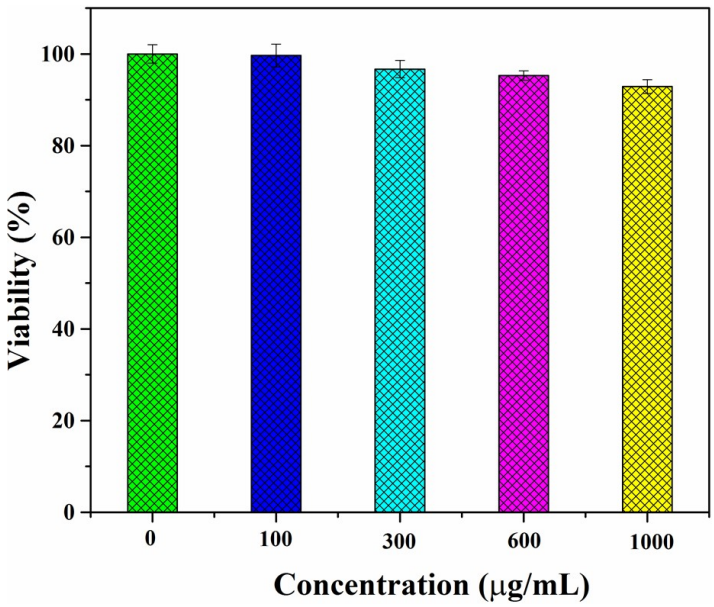

Figure S10. MTT assay for cell viability of Hek293 cells incubated with different concentrations of the modified X-PLNPs.

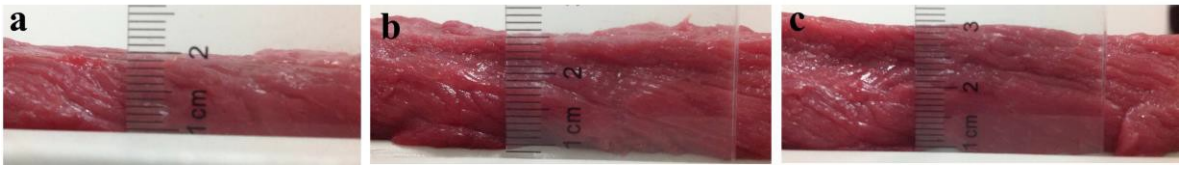

Figure S11. Digital pictures of different thicknesses of pork slabs: (a) 10 mm, (b) 15 mm, (c) 20 mm.

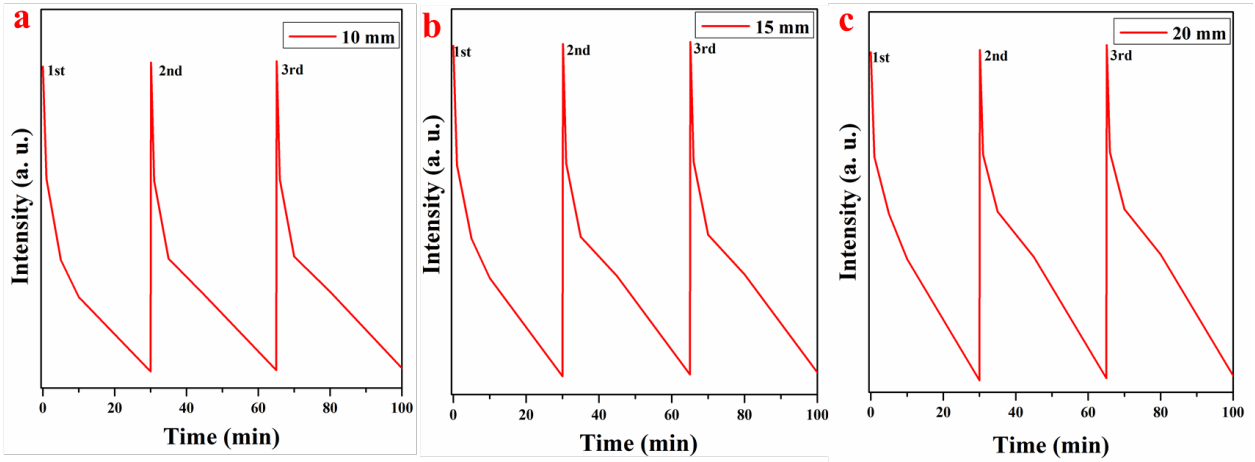

Figure S12. *In vivo* deep tissue NIR afterglow repeated imaging decay curves of a Kunming mouse after subcutaneous injection of X-PLNPs covered with different thicknesses of pork slabs (a) 10 mm, (b) 15 mm and (c) 20 mm after the stoppage of X-ray excitation.

Table S1. Illustration of penetration depth and different excitation source of optical nanoprobes.

Fluorescent Nanoprobe	Excitation Source	Depth [cm]	Reference
$ZnGa_2O_4Cr0.004$[a)]	white LED	1	[s1]
$NaYbF_4$: Tm[b)]	915 nm laser	1.75	[s2]
$NaYF_4$: Yb/Er[c)]	X-ray (320 kVp, 12.5 mA)		[s3]
$ZnGa_2O_4$: Cr	X-ray (45 kVp, 0.5 mA)	2	this work

[a)]$ZnGa_2O_4Cr_{0.004}$ PLNPs were pre-irradiated by white LED light and no illumination source was needed during imaging;[b)] *In vivo* imaging based on $NaYbF_4$: Yb/Tm upconversion nanoprobe was activated by 915 nm laser; [c)]Bioimaging based on $NaYF_4$: Yb/Er nanoprobe was irradiated by high-power X-ray source (320 kVp, 12.5 mA).

(s1) Li, Z. J.; Zhang, Y. W.; Wu, X.; Huang, L.; Li, D. S.; Fan, W.; Han, G. *J. Am. Chem. Soc.* **2015**, *137*, 5304.
(s2) Zhan, Q. Q.; Qian, J.; Liang, H. J.; Somesfalean, G.; Wang, D.; He, S.; Zhang, Z. G.; Andersson-Engels, S. *ACS. Nano.* **2011**, *5,* 3744.
(s3) Naczynski, D. J.; Sun, C.; Türkcan, S.; Jenkins, C.; Koh, A. L.; Ikeda, D.; Pratx, G.; Xing, L. *Nano Lett.* **2015**, *15*, 96.

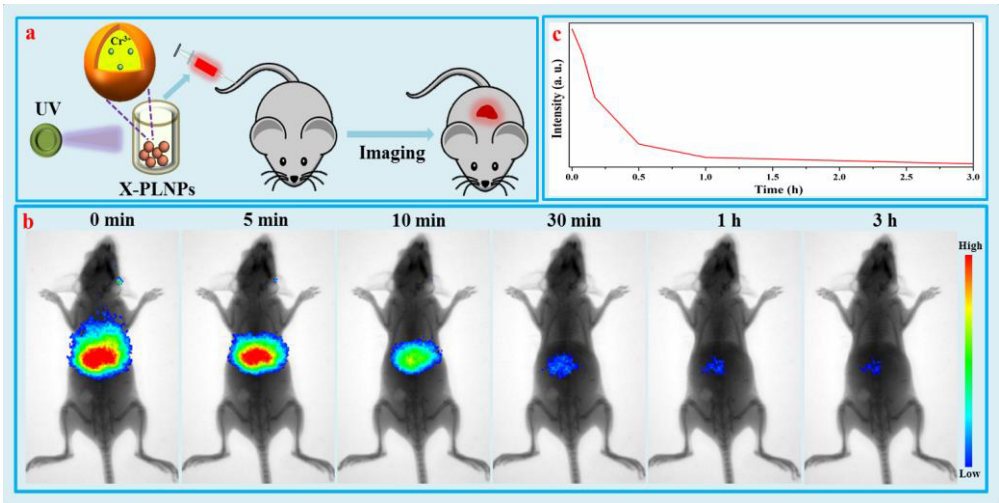

Figure S13. (a) A schematic representation of *in vivo* bioimaging of mouse after intravenous injection of X-PLNPs that irradiated by a UV lamp, (b) *in vivo* NIR persistent luminescence bioimaging and (c) the corresponding decay curves of a mouse after intravenously injected of X-PLNPs.

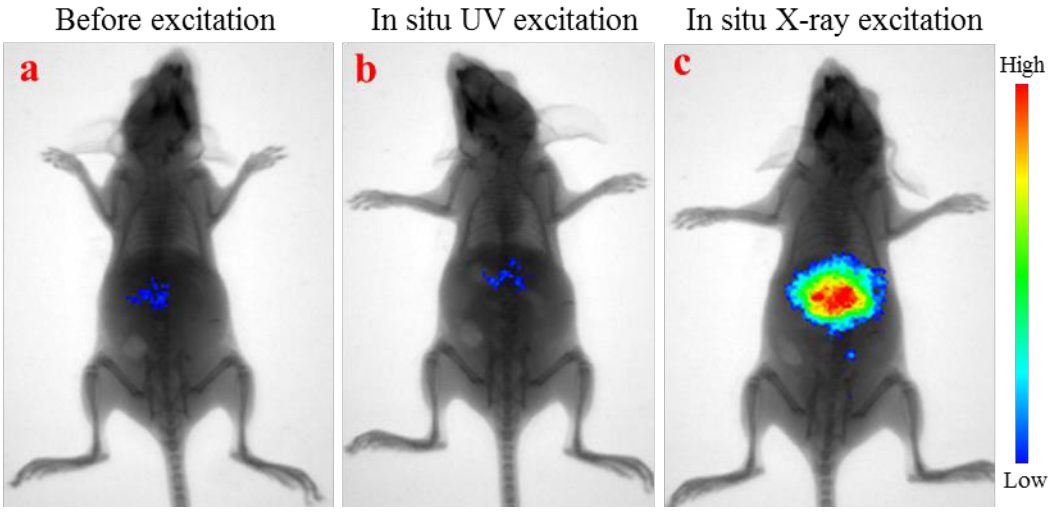

Figure S14. (a) *In vivo* decayed bioimaging of mouse after intravenous injection of X-PLNPs with *ex vivo* excitation by UV light, (b) *in vivo* renewable bioimaging of the mouse after in situ (b) UV and (c) X-ray excitation.

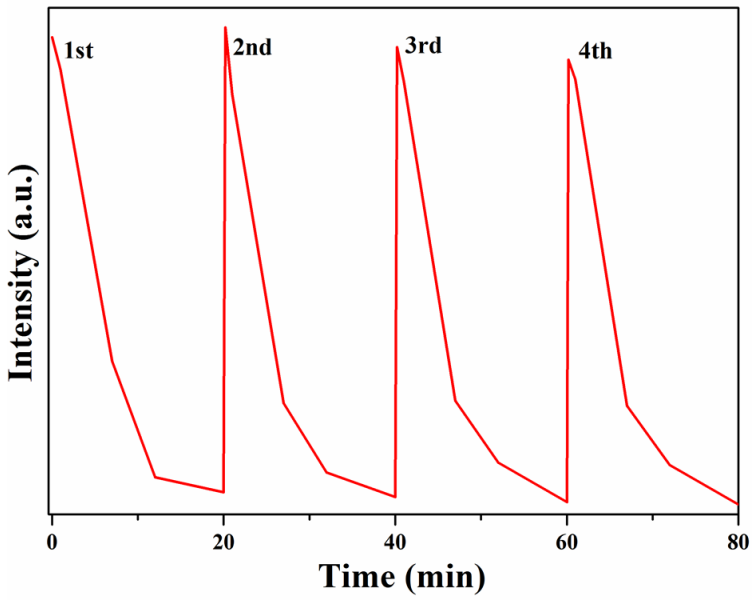

Figure S15. *In vivo* NIR persistent luminescence repeated imaging decay curves of a Kunming mouse after intravenous injection of X-PLNPs after X-ray excitation.

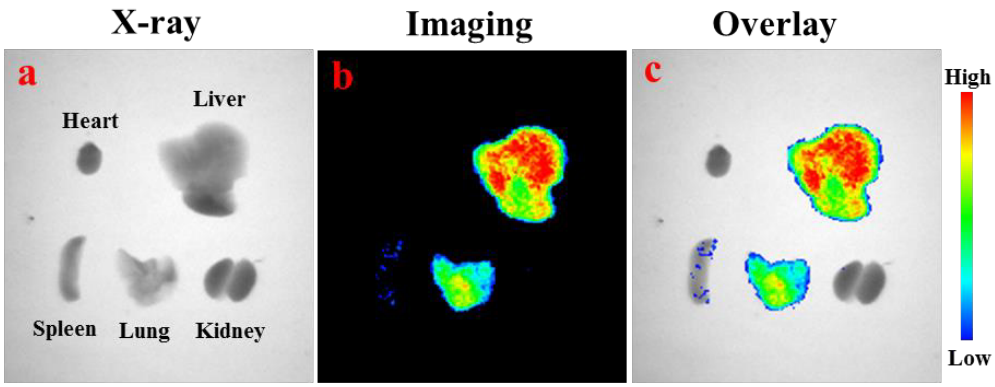

Figure S16. *Ex vivo* imaging of sacrificed organs (heart, liver, spleen, lung and kidney) obtained from the intravenously injected mouse after X-ray irradiation, a: X-ray images; b: persistent luminescence image; c: the overlay images.

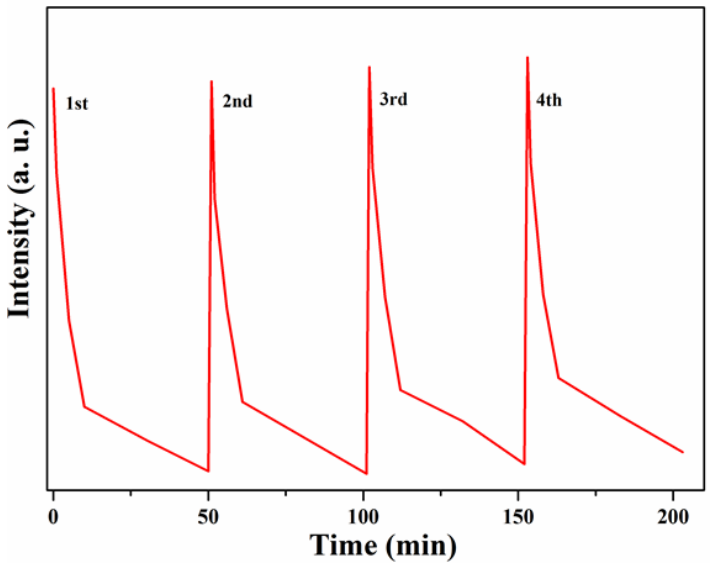

Figure S17. Decay curves of four repeated bioimaging of a Kunming mouse after oral administration of X-PLNPs after X-ray excitation.

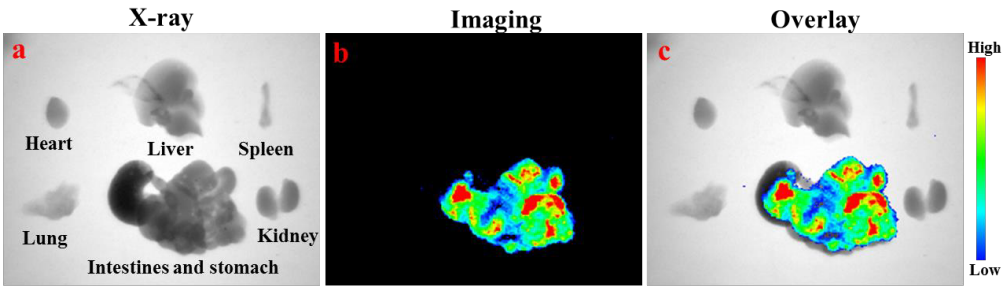

Figure S18. *Ex vivo* imaging of sacrificed organs (heart, liver, spleen, lung, intestines and stomach and kidney) achieved from the oral administrated mouse after X-ray excitation, a: X-ray images; b: NIR persistent luminescence image; c: the overlay images.